

Faddeev Equations for the  $K \rightarrow 3\pi$  Amplitude\*

I. M. BARBOUR† AND R. L. SCHULT

*Department of Physics, University of Illinois, Urbana, Illinois*

(Received 18 August 1966)

Integral equations for the three-pion decay amplitude of the  $K$  meson are derived in the context of a potential-scattering model. Nonlocal  $S$ - and  $P$ -wave separable potentials are used. Some numerical solutions are presented for the  $S$ -wave case. The shapes of the decay spectra are found to be insensitive to the shape of the potential for the cases investigated. The connection with the integral equations of Khuri and Treiman is discussed. A zero-range approximation requires that  $a_2^2 > a_0^2$  in order to fit the experimental data. Some aspects of three-body states in the presence of a resonance are investigated. No observable effects of a triangle singularity are found for the cases considered.

## INTRODUCTION

THE three-pion decay mode of the  $K$  meson has long been of interest because of the possible information it contains concerning the pion-pion interaction. Most previous analyses<sup>1-7</sup> of this decay have considered only the first rescattering of the pions in the final state and have neglected the effects of multiple scatterings which involve all three pions. The pion-pion scattering parameters obtained from such calculations (Ref. 4) generally disagree with the parameters obtained from other reactions both qualitatively and quantitatively.<sup>8,9</sup> This has led to the conclusion that the structure observed on the Dalitz plot for  $\tau$  decay is primarily a result of the weak interaction itself and not of the final-state pion-pion scattering.<sup>10,11</sup>

A gap in this argument is, of course, the neglect of the multiple scattering. Very little is known about three-body systems but recent work on triangle singularities,<sup>12,13</sup> overlapping resonances,<sup>14</sup> three-body unitarity, and other aspects<sup>15</sup> have indicated that there may be qualitatively new effects in a three-body system

not included in previous two-body calculations. Using the recent work of Faddeev<sup>16,17</sup> and of Hetherington and Schick<sup>18</sup> in nonrelativistic three-body systems, we investigate some of these effects in detail within the framework of a potential-scattering model.

In Sec. I we derive integral equations for the decay amplitudes. The final-state interactions are assumed to take place through a sum of two-body potentials. The equations are then specialized to the case of separable nonlocal  $S$ - and  $P$ -wave potentials. One choice for the form of the weak interaction is discussed in Sec. II A. The pion-pion potentials which we use, including one which can produce an  $S$ -wave resonance, are described in Sec. II B.

The equations derived in Sec. I are rewritten in Sec. III in a form suitable for numerical calculations. Numerical solutions for some simple cases are presented in Sec. IV under three categories. First, the dependence of the final Dalitz plot upon the potential shape is investigated briefly. Then, a comparison with the result of Khuri and Treiman<sup>1</sup> is made and the relationship between our equations and theirs is discussed. Finally, some aspects of three-body states in the presence of a two-particle resonance are investigated. Additional numerical work is in progress.

## I. INTEGRAL EQUATIONS FOR THE DECAY AMPLITUDE

The amplitude for  $K$ -meson decay into three pions can be expressed as

$$\langle \varphi_{3\pi} | U | \varphi_K \rangle = \langle \psi_{3\pi}^{(-)} | H_w | \varphi_K \rangle, \quad (1.1)$$

where  $H_w$  describes the purely weak interaction which initiates the decay. The final-state wave function for the three pions  $\psi_{3\pi}^{(-)}$  satisfies the equation appropriate

\* Work supported by the U. S. Office of Naval Research under Contract No. 1834(05).

† Present address: Physics Department, University of Sussex, Brighton, England.

<sup>1</sup> N. N. Khuri and S. B. Treiman, Phys. Rev. **119**, 1115 (1960).

<sup>2</sup> A. N. Mitra and Shubha Ray, Phys. Rev. **135**, 146 (1964).

<sup>3</sup> R. F. Sawyer and K. C. Wali, Phys. Rev. **119**, 1429 (1960).

<sup>4</sup> E. Lomon, S. Morris, E. J. Irwin, and T. Truong, Ann. Phys. (N. Y.) **13**, 359 (1961).

<sup>5</sup> M. A. B. Bég and P. C. DeCelles, Phys. Rev. Letters **8**, 46 (1962).

<sup>6</sup> L. M. Brown and P. Singer, Phys. Rev. Letters **8**, 460 (1962); Phys. Rev. **133**, B812 (1964).

<sup>7</sup> R. Prasad, Nuovo Cimento **35**, 682 (1965).

<sup>8</sup> L. T. Smith, D. J. Prowse, and D. H. Stork, Phys. Letters **2**, 204 (1962).

<sup>9</sup> J. Hamilton, P. Menotti, G. C. Oades, and L. L. J. Vick, Phys. Rev. **128**, 1881 (1962); N. Schmitz, Nuovo Cimento **31**, 255 (1964).

<sup>10</sup> Riazuddin and Fayyazuddin, Phys. Rev. Letters **7**, 464 (1961).

<sup>11</sup> G. Barton and C. Kacser, Phys. Rev. Letters **8**, 226 (1962).

<sup>12</sup> G. Barton and C. Kacser, Nuovo Cimento **21**, 593 (1961); I. P. Gzok and S. F. Tuan, *ibid.* **32**, 227 (1964); Y. F. Chang and S. F. Tuan, Phys. Rev. **136**, B741 (1964).

<sup>13</sup> I. J. R. Aitchison, Phys. Rev. **137**, B1070 (1965); I. J. R. Aitchison and C. Kacser, *ibid.* **142**, 1104 (1966).

<sup>14</sup> J. B. Bronzan, Phys. Rev. **134**, B687 (1964).

<sup>15</sup> R. Aaron, R. D. Amado, and Y. Y. Yam, Phys. Rev. **136**, B650 (1964); Phys. Rev. Letters **13**, 574 (1964); Phys. Rev. **140**, B1291 (1965).

<sup>16</sup> L. D. Faddeev, Zh. Eksperim. i Teor. Fiz. **39**, 1459 (1960) [English transl.: Soviet Phys.—JETP **12**, 1014 (1961)]; Dokl. Akad. Nauk SSSR **138**, 561 (1961); **145**, 301 (1962) [English transl.: Soviet Phys.—Doklady **6**, 384 (1961); **7**, 600 (1963)].

<sup>17</sup> C. A. Lovelace, Phys. Rev. **135**, B1225 (1964).

<sup>18</sup> J. H. Hetherington and L. H. Schick, Phys. Rev. **137**, B935 (1965); **139**, B1164 (1965); **141**, 1315 (1966).

for outgoing waves:

$$\begin{aligned} \langle \psi_{3\pi}^{(-)} | &= \langle \varphi_{3\pi} | + \langle \psi_{3\pi}^{(-)} | VG_0 \\ &= \langle \varphi_{3\pi} | + \langle \varphi_{3\pi} | TG_0, \end{aligned} \quad (1.2)$$

where  $\langle \varphi_{3\pi} |$  denotes plane waves and  $G_0$  is the free three-particle Green's function

$$G_0 = 1/(E - H_0 + i\epsilon), \quad \epsilon \rightarrow 0+ \quad (1.3)$$

where  $E$  is the total kinetic energy available ( $E = m_K - 3m_\pi$ ) and  $H_0$  is the three-particle kinetic-energy operator. The interaction of the pions (labeled  $i, j, k$ ;  $i \neq j \neq k$ ) is assumed to take place through a sum of two-body potentials

$$V = \sum_{i=1}^3 V_i, \quad (1.4)$$

where  $V_i$  is the potential between pions labeled  $j$  and  $k$ . The three-particle  $t$  matrix  $T$  satisfies the Lippmann-Schwinger equation

$$T = V + VG_0T. \quad (1.5)$$

Substitution of Eqs. (1.2) and (1.5) into Eq. (1.1) results in our basic equation for the decay. In operator form we obtain

$$\begin{aligned} U &= H_w + TG_0H_w \\ &= H_w + VG_0H_w + VG_0TG_0H_w \\ &= H_w + VG_0U. \end{aligned} \quad (1.6)$$

In order to eliminate the singular part of this equation we parallel the ideas of Faddeev<sup>16</sup> and define the three operators

$$U_i = V_i G_0 U, \quad i=1,2,3 \quad (1.7)$$

so that

$$U = H_w + \sum_i U_i. \quad (1.8)$$

The operators  $U_i$  then satisfy the coupled equations

$$U_i = V_i G_0 H_w + \sum_{j \neq i} V_j G_0 U_j + V_i G_0 U_i. \quad (1.9)$$

We now introduce operators  $t_i$  describing the (off-energy-shell) two-body scattering of pions  $j$  and  $k$  by the definition

$$t_i = V_i + V_i G_0 t_i. \quad (1.10)$$

Note that the pion labeled  $i$  enters Eq. (1.10) only through the energy denominator of  $G_0$ . In terms of these operators, Eq. (1.9) can be rewritten as

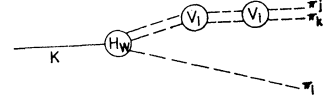
$$\begin{aligned} (1 - V_i G_0) U_i &= (1 - V_i G_0) t_i G_0 H_w \\ &+ (1 - V_i G_0) \sum_{j \neq i} t_j G_0 U_j, \end{aligned} \quad (1.11)$$

or

$$U_i = t_i G_0 H_w + \sum_{j \neq i} t_j G_0 U_j. \quad (1.12)$$

The inhomogeneous term in Eq. (1.12) sums all the perturbation diagrams in which pions  $j$  and  $k$  interact and

Fig. 1. An example of a perturbation diagram included in the first rescattering term.



pion  $i$  is a spectator (Fig. 1). This term is essentially the one used in some previous analyses<sup>6,7</sup> to estimate final-state interaction effects. We refer to it as the first rescattering term. It can be seen by iteration of Eq. (1.12) that the other terms (multiple-scattering terms) take into account all other graphs (i.e., those with no pion acting only as spectator—e.g., Fig. 2). Three-pion potentials are omitted, although they could be included if necessary.

Our next step is to specify the basis states in which to most conveniently express the matrix elements of the operators in Eq. (1.12). The general case of three particles of arbitrary mass and isospin is discussed by Hetherington and Schick.<sup>18</sup> Considerable simplification in the notation occurs for  $K$  decay if one neglects the pion mass differences and assumes that the weak interaction  $H_w$  obeys a  $|\Delta T| = \frac{1}{2}$  rule, since then the only important total isospin for the final state is  $T=1$ . With this restriction the three-pion state can be specified in the over-all center-of-mass frame by giving the total momentum  $\mathbf{q}_i$ , the relative momentum  $\mathbf{k}_i$ , and the isospin  $I$  of the pions labeled  $j$  and  $k$ . In terms of the momenta of the individual pions,  $\mathbf{P}_1, \mathbf{P}_2$ , and  $\mathbf{P}_3$ ,

$$\begin{aligned} \mathbf{q}_i &= \mathbf{P}_j + \mathbf{P}_k = -\mathbf{P}_i, \\ \mathbf{k}_i &= \frac{1}{2}(\mathbf{P}_k - \mathbf{P}_j), \quad i, j, k \text{ cyclic.} \end{aligned} \quad (1.13)$$

Since the basis  $|\mathbf{q}_j, \mathbf{k}_j, J\rangle$  is just as good as  $|\mathbf{q}_i, \mathbf{k}_i, I\rangle$ , we state the transformation matrices

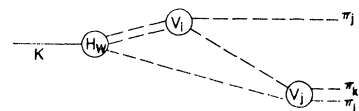
$$\begin{aligned} \langle \mathbf{q}_i, \mathbf{k}_i; I | \mathbf{q}_j, \mathbf{k}_j; J \rangle &= (2\pi)^3 \delta(\mathbf{q}_j + \frac{1}{2}\mathbf{q}_i - \mathbf{k}_i) \\ &\times (2\pi)^3 \delta(\mathbf{k}_j + \frac{3}{4}\mathbf{q}_i + \frac{1}{2}\mathbf{k}_i) R(I, J), \\ \langle \mathbf{q}_i, \mathbf{k}_i; I | \mathbf{q}_k, \mathbf{k}_k; K \rangle &= (2\pi)^3 \delta(\mathbf{q}_k + \frac{1}{2}\mathbf{q}_i + \mathbf{k}_i) \\ &\times (2\pi)^3 \delta(\mathbf{k}_k - \frac{3}{4}\mathbf{q}_i + \frac{1}{2}\mathbf{k}_i) R(I, K). \end{aligned} \quad (1.14)$$

The recoupling coefficients  $R(I, J) = (-1)^{I+J} R(J, I)$  are

$$\begin{bmatrix} \frac{1}{3} & +\frac{1}{3}\sqrt{3} & \frac{1}{3}\sqrt{5} \\ -\frac{1}{3}\sqrt{3} & -\frac{1}{2} & +\frac{1}{6}\sqrt{15} \\ \frac{1}{3}\sqrt{5} & -\frac{1}{6}\sqrt{15} & \frac{1}{6} \end{bmatrix}, \quad (1.15)$$

where rows and columns are the isospin in the order (0,1,2,) and  $i, j, k$  are cyclic.<sup>19</sup>

Fig. 2. An example of a perturbation diagram included in the multiple-scattering term.



<sup>19</sup> Our phase convention is slightly different from that of Hetherington and Schick (Ref. 18) in that cyclic order is preserved in all definitions. It is shown explicitly in Eq. (4.2).

The Green's function  $G_0$  can be written in any of the equivalent forms

$$G_0^{-1} = E - \frac{3}{4} \mathbf{q}_i^2 - \mathbf{k}_i^2 + i\epsilon, \quad \text{any } i \quad (1.16a)$$

or

$$G_0^{-1} = E - \mathbf{q}_i^2 - \mathbf{q}_i \cdot \mathbf{q}_j - \mathbf{q}_j^2 + i\epsilon, \quad \text{any } i \neq j \quad (1.16b)$$

(where the units  $m_\pi = c = \hbar = 1$  are used). Since the potential  $V_i$  conserves isospin and does not involve particle  $i$  we have

$$\langle \mathbf{k}_i, \mathbf{q}_i, I | V_i | \mathbf{k}'_i, \mathbf{q}'_i, I' \rangle = \delta_{II'} (2\pi)^3 \delta(\mathbf{q}_i - \mathbf{q}'_i) V(\mathbf{k}_i, \mathbf{k}'_i, I). \quad (1.17)$$

The matrix elements of Eq. (1.10) are then

$$\langle \mathbf{k}_i, \mathbf{q}_i, I | t_i | \mathbf{k}'_i, \mathbf{q}'_i, I' \rangle = \langle \mathbf{k}_i | t_i(\bar{q}_i, I) | \mathbf{k}'_i \rangle \delta_{II'} (2\pi)^3 \delta(\mathbf{q}_i - \mathbf{q}'_i), \quad (1.18)$$

$$U_i(\mathbf{k}_i, \mathbf{q}_i, I) = \int \frac{d^3 k'_i}{(2\pi)^3} \frac{\langle \mathbf{k}_i | t_i(\bar{q}_i, I) | \mathbf{k}'_i \rangle H_w(\mathbf{k}'_i, \mathbf{q}_i, I)}{E - \frac{3}{4} q_i^2 - k_i'^2 + i\epsilon} + \sum_J \int \frac{d^3 q'_j}{(2\pi)^3} \frac{\langle \mathbf{k}_i | t_i(\bar{q}_i, I) | \mathbf{q}'_j + \frac{1}{2} \mathbf{q}_i \rangle R(I, J) U_j(-\frac{1}{2} \mathbf{q}'_j - \mathbf{q}_i, \mathbf{q}'_j, J)}{E - q_i^2 - \mathbf{q}_i \cdot \mathbf{q}'_j - q_j'^2 + i\epsilon} + \sum_K \int \frac{d^3 q'_k}{(2\pi)^3} \frac{\langle \mathbf{k}_i | t_i(\bar{q}_i, I) | -\mathbf{q}'_k - \frac{1}{2} \mathbf{q}_i \rangle R(I, K) U_k(\frac{1}{2} \mathbf{q}'_k + \mathbf{q}_i, \mathbf{q}'_k, K)}{E - q_i^2 - \mathbf{q}_i \cdot \mathbf{q}'_k - q_k'^2 + i\epsilon}. \quad (1.22)$$

Since the pions are identical the particle labels  $i, j, k$  can be dropped temporarily.

Equation (1.22) is still too complicated to handle numerically because  $U(\mathbf{k}, \mathbf{q}, I)$  is a function of the three variables  $k^2, q^2$ , and  $\mathbf{k} \cdot \mathbf{q}$ . Further progress may be made by assuming that the potential  $V(\mathbf{k}, \mathbf{k}', I)$  can be approximated by a separable potential for each partial wave and keeping only the lowest partial wave for each value of  $I$ .<sup>20,21</sup>

$$V(\mathbf{k}, \mathbf{k}', I) = (2l+1) \lambda_I v_I(k) v_I(k') P_l(\hat{\mathbf{k}} \cdot \hat{\mathbf{k}}'), \quad (1.23)$$

with  $l=0$  for  $I=0, 2$  and  $l=1$  for  $I=1$  and  $v_I(k) \rightarrow k^l$  as  $k \rightarrow 0$  to insure the proper threshold behavior.

For this choice of potential the two-body  $t$ -matrix element in Eq. (1.19) also separates and is given by

$$\langle \mathbf{k} | t(\bar{q}, I) | \mathbf{k}' \rangle = (2l+1) v_I(k) v_I(k') P_l(\hat{\mathbf{k}} \cdot \hat{\mathbf{k}}') \tau(\bar{q}, I), \quad (1.24)$$

where

$$\tau^{-1}(\bar{q}, I) = \frac{1}{\lambda_I} \int \frac{d^3 k''}{(2\pi)^3} \frac{v_I^2(k'')}{\bar{q}^2 - k''^2 + i\epsilon}. \quad (1.25)$$

Now since the two-body  $t$  matrix is separable we see from Eq. (1.22) that  $U(\mathbf{k}, \mathbf{q}, I)$  is also separable:

$$U(\mathbf{k}, \mathbf{q}, I) = (2l+1) v_I(k) W(q, I) P_l(\hat{\mathbf{k}} \cdot \hat{\mathbf{q}}), \quad (1.26)$$

where the new function  $W(q, I)$  satisfies the integral equation

$$W(q, I) = \tau(\bar{q}, I) \left\{ F(\bar{q}, I) + \sum_J \int \frac{d^3 q'}{(2\pi)^3} K(\mathbf{q}, \mathbf{q}'; I, J) W(q', J) \right\}, \quad (1.27)$$

with

$$F(\bar{q}, I) = \int \frac{d^3 k'}{(2\pi)^3} \frac{v_I(k') P_l(\hat{\mathbf{k}}' \cdot \hat{\mathbf{q}}) H_w(\mathbf{k}', \mathbf{q}, I)}{\bar{q}^2 - k'^2 + i\epsilon}, \quad (1.28)$$

and

$$K(\mathbf{q}, \mathbf{q}', I, J) = \frac{v_I(k') P_l(\hat{\mathbf{q}} \cdot \hat{\mathbf{k}}') 2R(I, J) (2l+1) v_J(k'') P_l(\hat{\mathbf{k}}'' \cdot \hat{\mathbf{q}}')}{E - q^2 - \mathbf{q} \cdot \mathbf{q}' - q'^2 + i\epsilon}, \quad (1.29)$$

where

$$\langle \mathbf{k}_i | t_i(\bar{q}_i, I) | \mathbf{k}'_i \rangle = V(\mathbf{k}_i, \mathbf{k}'_i, I) + \int \frac{d^3 k''}{(2\pi)^3} \frac{V(\mathbf{k}_i, \mathbf{k}'', I) \langle \mathbf{k}'' | t_i(\bar{q}_i, I) | \mathbf{k}'_i \rangle}{\bar{q}_i^2 - \mathbf{k}''^2 + i\epsilon} \quad (1.19)$$

and

$$\bar{q}_i^2 = E - \frac{3}{4} \mathbf{q}_i^2. \quad (1.20)$$

Equation (1.19) is a standard integral equation for the two-pion scattering amplitude for incident relative momentum  $\mathbf{k}'_i$ , outgoing relative momentum  $\mathbf{k}_i$ , and relative energy  $\bar{q}_i^2$ .

Defining

$$\langle \mathbf{k}_i, \mathbf{q}_i, I | U_i | \varphi_K \rangle = U_i(\mathbf{k}_i, \mathbf{q}_i, I)$$

and

$$\langle \mathbf{k}_i, \mathbf{q}_i, I | H_w | \varphi_K \rangle = H_w(\mathbf{k}_i, \mathbf{q}_i, I), \quad (1.21)$$

we obtain from Eqs. (1.12), (1.14), (1.16), and (1.18)

<sup>20</sup> The validity of the separable approximation is discussed in many places, including Refs. 15 and 17.

<sup>21</sup> See also J. L. Basdevant and R. L. Omnès, Phys. Rev. Letters **17**, 775 (1966). Their caution against indiscriminate use of this approximation should be noted.

with  $\mathbf{k}' = \mathbf{q}' + \frac{1}{2}\mathbf{q}$  and  $\mathbf{k}'' = -\mathbf{q} - \frac{1}{2}\mathbf{q}'$ .

If the potentials  $v_I(k)$  are chosen to be simple enough, the integral in Eq. (1.28) and the angular integrations in Eq. (1.27) can be performed analytically, leaving a set of three coupled single-variable integral equations for the three functions  $W(q, I)$ . These equations consist of an inhomogeneous term describing the single rescattering and a "homogeneous" term describing multiple scattering.

The first rescattering term of Eq. (1.27) is not the same as used by Brown and Singer<sup>6</sup> and by Prasad.<sup>7</sup> The essential difference is the normalization. If only one isospin state is important, as in Ref. 6, this affects only the rate. However, when two or more channels are present, the relative normalization is important and the choice used by Prasad is not unique.

In the special case in which  $v_I(k) = \text{const}$  ( $v_I = 0$  for  $I = 1$ ), the various integrals diverge. However, we show in Sec. IV.B that in a once subtracted form Eq. (1.27) becomes identical to the equations derived by Anisovich,<sup>22</sup> which are in turn the same as the nonrelativistic limit of the Khuri-Treiman dispersion equations. Thus we expect that whenever the range of our potential is short, we should obtain the same results as would come from an exact solution of the Khuri-Treiman or Anisovich equations.

## II. SPECIFIC INTERACTIONS USED

### A. The Weak Interaction $H_w$

The spirit of final-state-interaction calculations is that all the observed energy dependence is assumed to be due to the final-state pion-pion interaction. In an attempt to be slightly more general, we have assumed that the weak interaction  $H_w$  may contribute terms which are constant or linear in the energy of each pion. Within the restrictions of Bose statistics and the  $|\Delta T| = \frac{1}{2}$  rule there are only two parameters in this description. The matrix elements  $\langle \mathbf{k}_i, \mathbf{q}_i, I | H_w | \varphi_K \rangle$  are

$$\begin{aligned} \langle \mathbf{k}_i, \mathbf{q}_i, 0 | H_w | \varphi_K \rangle &= \frac{1}{3}\sqrt{5}H - \frac{2}{3}\sqrt{3}A\left(\frac{1}{3}k_i^2 - \frac{1}{4}q_i^2\right), \\ \langle \mathbf{k}_i, \mathbf{q}_i, 1 | H_w | \varphi_K \rangle &= A\mathbf{k}_i \cdot \mathbf{q}_i, \\ \langle \mathbf{k}_i, \mathbf{q}_i, 2 | H_w | \varphi_K \rangle &= \frac{2}{3}H + \frac{1}{3}\sqrt{15}A\left(\frac{1}{3}k_i^2 - \frac{1}{4}q_i^2\right). \end{aligned} \quad (2.1)$$

Since we have

$$\frac{1}{3}k_i^2 - \frac{1}{4}q_i^2 = \frac{1}{3}(\mathbf{k}_j \cdot \mathbf{q}_j + \mathbf{k}_k \cdot \mathbf{q}_k), \quad (2.2)$$

the linear terms obey the above restrictions both on and off the energy shell.

In the absence of final-state interactions, a value of  $A/H$  between  $-0.33 m_\pi^{-2}$  and  $-0.46 m_\pi^{-2}$  would fit the observed energy spectra of  $K$  decay.

The numerical work reported in Sec. IV considers only the case  $A = 0$ .

### B. The Pion-Pion Potential

The low-energy pion-pion interaction is not very well known. For the  $P$  wave, the  $\rho$  resonance at 760 MeV presumably dominates. However,  $S$ -wave scattering lengths deduced from peripheral pion production ( $\pi^+p \rightarrow \pi^+\pi^+n$ , etc.)<sup>9</sup> disagree with those obtained from previous analyses of  $\tau$  decay. The Brown and Singer  $\sigma$  resonance<sup>6</sup> and various explanations of the ABC anomaly<sup>23</sup> have also been proposed but no consistent scheme has yet been devised. Indeed, it is not even clear whether the  $S$ -wave pion-pion potential is attractive or repulsive.<sup>24</sup>

The  $S$ -wave potential we use has sufficient flexibility to generate a resonance or a zero effective range as well as the more usual  $S$ -wave behavior. In momentum space we choose

$$\begin{aligned} v(\mathbf{k}, \mathbf{k}', I) &= \lambda_I v_I(k) v_I(k'), \\ v_I(k) &= 1/(k^2 + \beta_I^2)(k^2 + \beta_I^{*2}), \quad \text{Re}\beta_I > 0. \end{aligned} \quad (2.3)$$

This corresponds to a separable potential in position space of the form

$$v_I(r, r') = \lambda' \left( \frac{e^{-ar} \sin br}{br} \right) \left( \frac{e^{-ar'} \sin br'}{br'} \right), \quad (2.4)$$

with  $\beta_I = a + ib$ . The oscillations of the sine function seem to provide sufficient barriers to allow an  $S$ -wave resonance to occur. We refer to this potential as the potential CP (for "complex parameter").

The  $t$  matrix generated by this potential is

$$\begin{aligned} \langle \mathbf{k} | t(\bar{q}, I) | \mathbf{k}' \rangle &= v_I(k) \tau(\bar{q}, I) v_I(k'), \\ \tau^{-1}(\bar{q}, I) &= \frac{1}{\lambda_I} \\ &= \frac{(\bar{q}^2 + 4i \text{Re}\beta_I \bar{q} - \beta_I^2 - 3|\beta_I|^2 - \beta_I^{*2})}{(\beta_I - i\bar{q})^2 (\beta_I^* - i\bar{q})^2 8\pi (\beta_I + \beta_I^*)^3 |\beta_I|^2}. \end{aligned} \quad (2.5)$$

The on-shell amplitude has a scattering length and effective range

$$\begin{aligned} \frac{1}{a_I} &= \frac{4\pi |\beta_I|^8}{\lambda_I} + \frac{|\beta_I|^2 (\beta_I^{*2} + 3|\beta_I|^2 + \beta_I^2)}{2(\beta_I + \beta_I^*)^3}, \\ r_I &= -\frac{16\pi |\beta_I|^4 (\beta_I^2 + \beta_I^{*2})}{\lambda_I} \\ &+ \frac{(\beta_I^{*4} + 3(\beta_I^{*2} + \beta_I^2) |\beta_I|^2 + 7|\beta_I|^4 + \beta_I^4)}{|\beta_I|^2 (\beta_I + \beta_I^*)^3}, \end{aligned} \quad (2.6)$$

where

$$t^{-1}(\bar{q}, I) = -(1/4\pi) \{ -i\bar{q} - 1/a_I + \frac{1}{2}r_I \bar{q}^2 + O(\bar{q}^4) \}.$$

<sup>22</sup> V. V. Anisovich, Zh. Eksperim. i Teor. Fiz. 44, 1593 (1963) [English transl.: Soviet Phys.—JETP 17, 1072 (1963)].

<sup>23</sup> A. Abashian, N. E. Booth, K. M. Crowe, R. E. Hill, and E. H. Rogers, Phys. Rev. 132, 2296 (1963).

<sup>24</sup> G. F. Chew, Phys. Rev. Letters 16, 60 (1966).

By varying the parameters  $\lambda_I$  and  $\beta_I$ , we can adjust this potential to lead to either a resonance or a bound state in the  $S$ -wave pion-pion system. Knowledge of only the scattering length and either the effective range or bound-state energy of the scattering amplitude is sufficient to determine only two of the three parameters associated with this potential. The third parameter, which we take to be the phase of  $\beta$ , can be partially restricted in its possible range of values by requiring that the coefficients of  $\bar{q}^4$ ,  $\bar{q}^6$ , and  $\bar{q}^8$  in  $t^{-1}(\bar{q}, I)$  be relatively small. Also, the structure of the final integral equation leading to the  $K \rightarrow 3\pi$  decay amplitude is such that the numerical method of solution is easier and faster if the phase of  $\beta$  is small [see Eq. (3.12)].

For the cases of interest, summarized below, the parameters were determined:

(1) In the case of a resonance, by fixing the scattering length, resonance energy and resonance width.

(2) In the case of a bound state, by fixing the mass of the bound state and the scattering length. The phase of  $\beta$  is arbitrary. The choice  $\text{Re}\beta_I = \sqrt{2} \text{Im}\beta_I$  satisfied the above conditions for the cases considered and was adopted in the numerical calculations.

(3) In the case of no resonance or bound state, by fixing the scattering length and effective range. For the cases considered, except for zero effective range, it was again found convenient to choose

$$\text{Re}\beta_I = \sqrt{2} \text{Im}\beta_I.$$

(4) In the case of zero effective range, by fixing the scattering length  $a$ . Then

$$\lambda = \frac{16\pi(\beta + \beta^*)^3(\beta^2 + \beta^{*2})|\beta|^6}{\beta^4 + 3|\beta|^2(\beta^2 + \beta^{*2}) + 7|\beta|^4 + \beta^{*4}}$$

and

$$\frac{1}{a} = \frac{|\beta|^2(3\beta^4 + 9|\beta|^2(\beta^2 + \beta^{*2}) + 11|\beta|^4 + 3\beta^{*4})}{4(\beta + \beta^*)^3(\beta^2 + \beta^{*2})},$$

and some added restrictions can be placed on the phase of  $\beta$ . For an attractive potential

$$a > 0 \text{ implies } (\text{Im}\beta)^2 > (2\sqrt{21} - 7)(\text{Re}\beta)^2,$$

$$a < 0 \text{ implies } (\text{Re}\beta)^2 < (\text{Im}\beta)^2 < (2\sqrt{21} - 7)(\text{Re}\beta)^2,$$

and for a repulsive potential

$$a > 0, \text{ and } \text{Im}\beta < \text{Re}\beta.$$

The choices of phases used were

$$\text{Im}\beta = (\sqrt{2.4}) \text{Re}\beta, \quad a > 0, \quad \text{attractive potential};$$

$$\text{Im}\beta = \sqrt{2} \text{Re}\beta, \quad a < 0, \quad \text{attractive potential};$$

$$\text{Im}\beta = 0.1 \text{Re}\beta, \quad a > 0, \quad \text{repulsive potential};$$

and are such that the coefficients of  $\bar{q}^4$ ,  $\bar{q}^6$ , and  $\bar{q}^8$  in  $t^{-1}(\bar{q}, I)$  are small except for the case of a repulsive potential.

In order to investigate the dependence of the final theoretical spectra upon the choice of potential we also considered the  $S$ -wave nonlocal separable potential (referred to as RP for "real parameter")

$$v(k, k', I) = \lambda_I v_I(k) v_I(k'); \quad v_I(k) = 1/(k^2 + \beta_I^2), \\ \beta_I \text{ real and } > 0. \quad (2.7)$$

This potential leads to a scattering amplitude

$$\langle k | t(\bar{q}, I) | k' \rangle = v_I(k) v_I(k') \\ \times \{1/\lambda_I + 1/8\pi\beta_I(\beta_I - i\bar{q})^2\}^{-1}, \quad (2.8)$$

which cannot resonate. Comparisons were made for cases (2) and (3).

For the  $P$  wave we choose

$$v(\mathbf{k}, \mathbf{k}', I) = 3\lambda_I v_I(k) (\hat{\mathbf{k}} \cdot \hat{\mathbf{k}}') v_I(k'), \quad (2.9)$$

with

$$v_I(k) = k/(k^2 + \beta_I^2)(k^2 + \beta_I^{*2}). \quad (2.10)$$

The  $t$  matrix which results is

$$\langle \mathbf{k} | t(\bar{q}, I) | \mathbf{k}' \rangle = 3v_I(k) \hat{\mathbf{k}} \cdot \hat{\mathbf{k}}' v_I(k') \tau(\bar{q}, I),$$

where

$$\tau^{-1}(\bar{q}, I) = \frac{1}{\lambda_I} \frac{1}{8\pi} \frac{\bar{q}^2 + 2i\bar{q}(\beta_I + \beta_I^*) - \beta_I\beta_I^*}{(\beta_I + \beta_I^*)^3(\beta_I - i\bar{q})^2(\beta_I^* - i\bar{q})^2}. \quad (2.11)$$

The on-shell effective-range expansion is then

$$k^3 \cot\delta = -\frac{4\pi}{\lambda} |\beta|^8 - \frac{|\beta|^6}{16(\text{Re}\beta)^3} + k^2 \left\{ -\frac{8\pi}{\lambda} |\beta|^4(\beta^2 + \beta^{*2}) \right. \\ \left. - \frac{3|\beta|^2(\beta^2 + \beta^{*2} + |\beta|^2)}{16(\text{Re}\beta)^3} \right\} + O(k^4). \quad (2.12)$$

For  $\lambda = -0.1721 \times 10^9$ ,  $\beta = 15.0 + 6.49i$  we can obtain a resonance at a mass = 763 MeV with width  $\Gamma = 100$  MeV.

The functions  $F(\bar{q}, I)$  corresponding to these potentials are

$$F(\bar{q}, 0) = -\frac{1}{4\pi} \frac{1}{\beta_0 + \beta_0^*} \frac{1}{(\beta_0 - i\bar{q})} \frac{1}{(\beta_0^* - i\bar{q})} \left[ +\frac{1}{3}\sqrt{5}H \right. \\ \left. + (2/3\sqrt{3})A[E - \bar{q}^2 - \beta_0\beta_0^* + i\bar{q}(\beta_0 + \beta_0^*)] \right], \\ F(\bar{q}, 1) = -\frac{1}{4\pi} \frac{1}{\beta_1 + \beta_1^*} \frac{1}{\beta_1 - i\bar{q}} \frac{1}{\beta_1^* - i\bar{q}} \\ \times \frac{1}{3}A[\beta_1\beta_1^* - i\bar{q}(\beta_1 + \beta_1^*)]q, \\ F(\bar{q}, 2) = -\frac{1}{4\pi} \frac{1}{\beta_2 + \beta_2^*} \frac{1}{\beta_2 - i\bar{q}} \frac{1}{\beta_2^* - i\bar{q}} \left[ +\frac{2}{3}H \right. \\ \left. - (\sqrt{5}/3\sqrt{3})A[E - \bar{q}^2 - \beta_2\beta_2^* + i\bar{q}(\beta_2 + \beta_2^*)] \right], \quad (2.13)$$

for the oscillating potential CP.

The linear coefficient  $A$  must be set equal to zero for the simpler potential RP to make the integrals

convergent. We then have

$$\begin{aligned} F(\bar{q}, 0) &= -\frac{1}{4\pi} \frac{1}{\beta_0 - i\bar{q}} \left( +\frac{\sqrt{5}}{3} H \right), \\ F(\bar{q}, 2) &= -\frac{1}{4\pi} \frac{1}{\beta_2 - i\bar{q}} \left( +\frac{2}{3} H \right). \end{aligned} \quad (2.14)$$

### III. METHOD OF SOLUTION

The forms chosen in Sec. II for the potential allow the angular integrations of Eq. (1.27) to be performed leading to a set of three coupled one-dimensional integral equations of the form

$$W(q, I) = W_0(q, I) + \sum_J \int_0^\infty dq' \bar{K}(q, q'; I, J) W(q', J), \quad (3.1)$$

where

$$W_0(q, I) = \tau(\bar{q}, I) F(\bar{q}, I), \quad (3.2)$$

and

$$\begin{aligned} \bar{K}(q, q'; I, J) &= -\frac{q'}{q} \frac{\tau(\bar{q}, I)}{(2\pi)^2} \\ &\times \sum_{i=1}^N \frac{A(I, J) \alpha_i^2 + B(I, J) \alpha_i + C(I, J)}{\prod_{j \neq i} (\alpha_j - \alpha_i)} \times \ln \frac{\alpha_i + qq'}{\alpha_i - qq'}. \end{aligned} \quad (3.3)$$

In Eq. (3.3),  $N$  is 3 or 5 depending on which potential is used:

$$\begin{aligned} \alpha_1 &= -E + q^2 + q'^2, \\ \alpha_2 &= q'^2 + \frac{1}{4}q^2 + \beta_I^2, \\ \alpha_3 &= \frac{1}{4}q'^2 + q^2 + \beta_J^2, \\ \alpha_4 &= q'^2 + \frac{1}{4}q^2 + \beta_I^{*2}, \\ \alpha_5 &= \frac{1}{4}q'^2 + q^2 + \beta_J^{*2}, \end{aligned} \quad (3.4)$$

and the matrices  $A$ ,  $B$ , and  $C$  are

$$\begin{aligned} A &= \begin{pmatrix} 0 & 0 & 0 \\ 0 & 3/qq' & 0 \\ 0 & 0 & 0 \end{pmatrix}, \\ B &= \begin{pmatrix} 0 & \frac{2\sqrt{3}}{q'} & 0 \\ +\frac{2}{\sqrt{3}q} & -\frac{3}{2} \left( \frac{q'}{q} + \frac{q}{q'} \right) & -\left( \sqrt{\frac{5}{3}} \right) \frac{1}{q} \\ 0 & -\frac{\sqrt{15}}{q'} & 0 \end{pmatrix}, \\ C &= \begin{pmatrix} \frac{2}{3} & -\sqrt{3}q' & \frac{2}{3}\sqrt{5} \\ -\frac{1}{3}q\sqrt{3} & \frac{3}{4}qq' & \frac{1}{6}q\sqrt{15} \\ \frac{2}{3}\sqrt{5} & \frac{1}{2}q'\sqrt{15} & \frac{1}{3} \end{pmatrix}. \end{aligned} \quad (3.5)$$

The procedure used for solving Eq. (3.1) is the same as that outlined by Hetherington and Schick.<sup>18</sup>

The kernel  $\bar{K}(q, q'; I, J)$  has logarithmic singularities at

$$\begin{aligned} q' &= \pm \frac{1}{2}q \pm i\beta_I; & q' &= \pm \frac{1}{2}q \pm i\beta_I^*; \\ q' &= \pm 2q \pm 2i\beta_J; & q' &= \pm 2q \pm 2i\beta_J^*; \end{aligned} \quad (3.6)$$

and

$$q' = \pm \frac{1}{2}q \pm (E - \frac{3}{4}q^2 + i\epsilon)^{1/2},$$

together with square-root singularities at

$$q = \pm \left[ \frac{4}{3}(E + i\epsilon) \right]^{1/2}$$

and other singularities of  $\tau(\bar{q}, I)$ .

For  $q$  real, the Green's-function singularities at

$$q' = \pm \frac{1}{2}q \pm (E - \frac{3}{4}q^2 + i\epsilon)^{1/2} \quad (3.7)$$

lie in the region of integration. These singularities can be avoided by rotating the variables  $q$  and  $q'$  simultaneously into the fourth quadrant of their complex planes, i.e.,

$$q = ye^{-i\Phi}; \quad q' = xe^{-i\Phi}; \quad x, y \text{ real and } \geq 0. \quad (3.8)$$

We are free to make this rotation as long as the contribution from the arc at infinity is zero and the integration contour ( $0 \leq x \leq \infty$ ) does not cross a singularity of the integrand. Then the integral Eq. (3.1) becomes

$$\begin{aligned} W(y e^{-i\Phi}, I) &= W_0(y e^{-i\Phi}, I) + \sum_J \int_0^\infty dx \\ &\times e^{-i\Phi} \bar{K}(y e^{-i\Phi}, x e^{-i\Phi}; I, J) W(x e^{-i\Phi}, J). \end{aligned} \quad (3.9)$$

From Eq. (3.6) we see that as we rotate the integration contour, the first singularity of the kernel to be encountered is at

$$\Phi_1 = \tan^{-1}(\text{Re}\beta / |\text{Im}\beta|).$$

The functions  $\tau(\bar{k}, I)$  and  $F(\bar{k}, I)$  with

$$\bar{k} = (E - \frac{3}{4}y^2 e^{-2i\Phi})^{1/2}$$

are not singular in the region  $0 < \Phi < \frac{1}{2}\pi$  for the potentials under consideration.

Numerical solution of Eq. (3.9) for  $W(ye^{-i\Phi}, I)$  is now straightforward. However, in order to find  $W(q, I)$  for  $q$  real, we have to rotate the complex variable  $q$  back to the real axis in Eq. (3.9). This is equivalent to rotating only the integration variable  $q'$  into the fourth quadrant of its complex plane through the angle  $\Phi$  in Eq. (3.8).

However, some care is required. For  $q$  real and greater than  $\sqrt{E}$  the singularity of the kernel at

$$q' = q_s' = \frac{1}{2}q - (E - \frac{3}{4}q^2 + i\epsilon)^{1/2}$$

lies just below the real positive  $q'$  axis complicating the rotation of contour. A suitable choice of contours<sup>25</sup> is

<sup>25</sup> J. H. Hetherington (private communication).

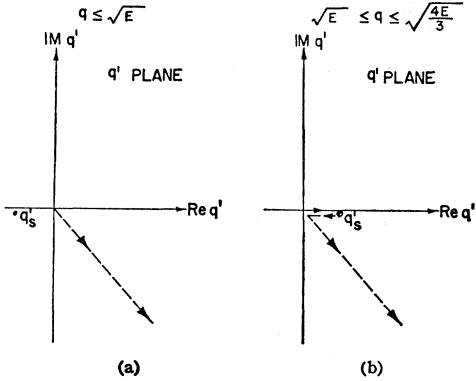


FIG. 3. Integration contours used in obtaining Eq. (3.10).

shown in Figs. 3(a) and 3(b). Then

$$W(q, I) = W_0(q, I) + \sum_J \int_0^\infty dx e^{-i\Phi} \bar{K}(q, x e^{-i\Phi}; I, J) \times W(x e^{-i\Phi}, J) + \int_0^{\frac{1}{2}q - \sqrt{(E - \frac{3}{4}q^2)}} dq' \Delta \bar{K}(q, q'; I, J) \times W(q', J) \theta(q - \sqrt{E}), \quad (3.10)$$

where the discontinuity of the kernel around the logarithmic branch point at  $q_s'$  is

$$\Delta \bar{K}(q, q'; I, J) = +(iq'/2\pi q) \tau(\bar{q}, I) v_I(\bar{q}) [A(I, J) \alpha_1^2 + B(I, J) \alpha_1 + C(I, J)] v_J((E - \frac{3}{4}q'^2)^{1/2}). \quad (3.11)$$

With this choice of contour, the kernel becomes singular first at

$$\Phi_q = \tan^{-1}(\text{Re}\beta_J / (q + |\text{Im}\beta_J|))$$

for each value of  $q$ . Hence Eqs. (3.9) and (3.10) result from valid contour rotations if we choose

$$0 < \Phi < \Phi_{\max}, \quad (3.12)$$

where  $\Phi_{\max}$  is the smallest value of  $\Phi_q$  for  $J=0, 1, 2$  and for  $0 \leq q \leq (4E/3)^{1/2}$  (the physical region for  $K$  decay).

A further change of variables was made in Eqs. (3.9) and (3.10) in order to make the integration regions finite:

$$x = \alpha s / (1-s), \quad y = \alpha t / (1-t). \quad (3.13)$$

The parameter  $\alpha$  was used to position the dominant part of the integrands near the middle of the integration range 0 to 1.

It was also found to be convenient (when  $A=0$ ) to solve for the functions

$$Z(t, I; \alpha, \Phi) = \frac{\alpha t e^{-i\Phi}}{1-t} W\left(\frac{\alpha t e^{-i\Phi}}{1-t}, I\right). \quad (3.14)$$

This simplifies the numerical calculation of the kernel at the endpoints of the integration.

With the above modifications, Eq. (3.1) takes the

final form amenable for numerical calculation:

$$Z(t, I; \alpha, \Phi) = Z_0(t, I; \alpha, \Phi) + \sum_J \int_0^1 \frac{\alpha t e^{-i\Phi}}{s(1-s)(1-t)} \times \bar{K}\left(\frac{\alpha t e^{-i\Phi}}{1-t}, \frac{\alpha s e^{-i\Phi}}{1-s}; I, J\right) Z(s, J; \alpha, \Phi) ds, \quad (3.15)$$

and

$$W(q, I) = W_0(q, I) + \sum_J \int_0^1 \frac{1}{s(1-s)} K\left(q, \frac{\alpha s e^{-i\Phi}}{1-s}; I, J\right) \times Z(s, J; \alpha, \Phi) ds + \theta(q - \sqrt{E}) \times \sum_J \int_0^{\frac{1}{2}q - \sqrt{(E - \frac{3}{4}q^2)}} dq' \Delta \bar{K}(q, q'; I, J) W(q', J). \quad (3.16)$$

For  $q > \sqrt{E}$ , Eq. (3.16) requires knowledge of  $W(q', J)$  for  $q' < \sqrt{(E/3)}$ . Hence we first evaluate Eq. (3.16) for  $q < \sqrt{E}$  and use these results in computing  $W(q, I)$  for  $q > \sqrt{E}$ .

The last term of Eq. (3.16) is particularly important when  $\tau(\bar{q}, I)$  has a narrow resonance for  $\bar{q}^2$  between  $\frac{3}{4}E$  and  $E$ . In this case the endpoint  $q_s'$  of the integral passes very close to the resonance pole in  $W(q', J)$ . The resulting logarithmic singularity<sup>13</sup> at

$$q = \frac{1}{2}q_r + k_r; \quad k_r^2 = E - \frac{3}{4}q_r^2 = m_{\text{res}} - 2 - i\frac{1}{2}\Gamma_{\text{res}}$$

corresponds to the triangle singularity of amplitudes such as that illustrated in Fig. 4. The effect of this singularity will be discussed later.

Equation (3.15) was solved by matrix inversion on an IBM 7094 computer. The angle  $\Phi$  was taken to be  $0.5 \Phi_{\max}$  and the parameter  $\alpha$  was chosen to make the dominant structure of the solution  $Z(t, I; \alpha, \Phi)$  occur near  $t = \frac{1}{2}$ . A mesh of between 25 and 45 points was found to be sufficiently accurate. For those potentials leading to a kernel with rapid variations, the mesh size was increased in order to check the accuracy of the solution.

For the case in which a pion-pion scattering amplitude resonates, the imaginary part of  $\beta$  (which determines the oscillatory nature of the potential) is large compared with the real part. Thus  $\Phi_{\max}$  is small ( $\sim 0.1$  rad) and rotation of the contours through an angle  $0.5\Phi_{\max}$  does not make the singularities of the kernel very distant. However, even in this case, a mesh of 45 points was more than sufficient.

Since the kernel of Eq. (3.16) is more singular than that of Eq. (3.15), we interpolated the function  $Z(t, I; \alpha, \Phi)$  (in general found to be a smooth function) using a seven-point Lagrange interpolation formula,

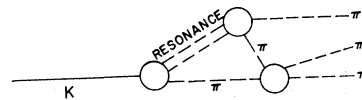


FIG. 4. An example of a graph in the multiple-scattering series which can contain a triangle singularity.

thus tripling the number of points at which the integrand in Eq. (3.16) can be evaluated. If this procedure is not followed, then more mesh points in Eq. (3.15) are needed in order to obtain  $W(q, I)$  to the same accuracy.

#### IV. RESULTS

The differential decay rate is proportional to the square of the matrix element of Eqs. (1.1) and (1.8):

$$|M|^2 = |\langle \varphi_{3\pi} | H_w + \sum_{i=1}^3 U_i | \varphi_K \rangle|^2. \quad (4.1)$$

Specifying pions 1, 2, and 3 to have charges  $m_1, m_2,$  and  $m_3,$  respectively, we expand the state  $\langle \varphi_{3\pi} | = \langle m_1, m_2, m_3 |$  in terms of our set of basis states, i.e.,

$$\langle m_1, m_2, m_3 | = \sum_{I=0}^2 C(1, 1, I; m_j, m_k) \times C(1, I, 1; m_i, m_j + m_k) \langle \mathbf{q}_i, \mathbf{k}_i, I |, \quad (4.2)$$

where the  $C$ 's are Clebsch-Gordan coefficients and the index  $i$  may be 1, 2, or 3, and  $i, j, k$  are cyclic. We choose the pion labeled 3 to be the odd pion for  $K^\pm$  decay and the  $\pi^0$  for  $K^0_2$  decay. The matrix element  $M$  is then

$$M = \sum_{i=1}^3 \sum_{I=0}^2 \{ H_w(\mathbf{k}_3, \mathbf{q}_3, I) \delta_{i3} + U_i(\mathbf{k}_i, \mathbf{q}_i, I) \} \times C(1, 1, I; m_j, m_k) C(1, I, 1; m_i, m_j + m_k), \quad (4.3)$$

where we have used Eq. (1.21). The functions  $H_w(\mathbf{k}, \mathbf{q}, I)$  and  $U(\mathbf{k}, \mathbf{q}, I)$  are given by Eqs. (2.1) and (1.26), respectively.

The differential decay rate is a function of only two variables which we choose to be the Dalitz variables<sup>26</sup>

$$x = \sqrt{3}(P_1^2 - P_2^2)/2E = -\sqrt{3}\mathbf{q}_3 \cdot \mathbf{k}_3/E,$$

and

$$y = 3P_3^2/2E - 1 = 3q_3^2/2E - 1. \quad (4.4)$$

The physical values of  $x$  and  $y$  are therefore

$$x^2 + y^2 \leq 1. \quad (4.5)$$

As is usual, we present our results in terms of the spectra  $X(x)$  and  $Y(y)$  which are  $|M(x, y)|^2$  averaged over allowed values of  $y$  and  $x$ , respectively, i.e.,

$$X(x) = \frac{\int_{-\sqrt{1-x^2}}^{\sqrt{1-x^2}} |M(x, y)|^2 dy}{2\sqrt{1-x^2}}, \quad (4.6)$$

and

$$Y(y) = \frac{\int_{-\sqrt{1-y^2}}^{\sqrt{1-y^2}} |M(x, y)|^2 dx}{2\sqrt{1-y^2}}.$$

The symmetry between pions 1 and 2 requires that  $X(x)$  be an even function of  $x$ . Since we cannot calculate absolute rates, we plot  $X(x)/X(0)$  and  $Y(y)/Y(0)$ .

The experimental data<sup>27</sup> are consistent with

$$X(x)/X(0) = 1 \quad \text{and} \quad Y(y)/Y(0) = 1 + \alpha y, \quad (4.7)$$

where  $\alpha$  is about 0.23 for  $K^+ \rightarrow \pi^+\pi^+\pi^-$ , and  $\alpha$  is about  $-0.63$  for  $K^+ \rightarrow \pi^0\pi^0\pi^+$  and  $K^0_1 \rightarrow \pi^+\pi^-\pi^0$ .

#### A. Comparison of Potentials

A large class of potentials will generate the same low-energy pion-pion scattering amplitude. These potentials differ in their high-energy and off-energy-shell behavior. Since the Faddeev equations depend on the off-shell behavior of the scattering amplitude, the energy spectra obtained may be sensitive to the shape of the potential chosen. Hence, as a preliminary step we calculated the three-pion-decay Dalitz plots for two different potentials which give the same scattering length and effective range. The potentials used are CP and RP, described in Sec. II. One noticeable difference in the potentials is the different shape for large  $k^2$ . This leads essentially to a different cutoff in the integrals of the equations.

The results are shown in Figs. 5–8 for the complete solution  $W(q, I)$  to Eqs. (3.15) and (3.16) and for the first rescattering approximation  $W(q, I) \cong W_0(q, I)$ . For the complete solution, the spectra are very nearly independent of which potential is chosen. The first rescattering terms differ somewhat more but the effect of multiple rescattering is more important than the difference between the potentials.

The spectra of Figs. 5 and 6 are dominated by the presence of an  $I=0$  bound state at  $1.91 m_\pi$ . The cusp at

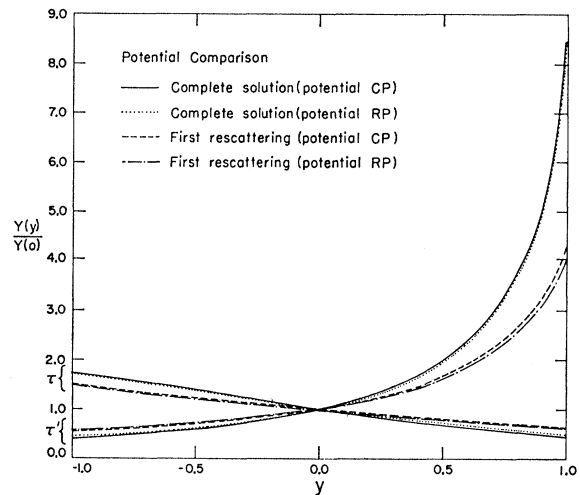


FIG. 5. The normalized decay spectra  $Y(y)/Y(0)$  for  $a_0 = 4.22 m_\pi^{-1}$  and a bound state at  $1.91 m_\pi$ , no  $I=1$  or 2 amplitudes, and  $A=0$ .

<sup>27</sup> G. H. Trilling, in Proceedings of the Argonne International Conference on Weak Interactions, 1965, Argonne National Laboratory Report No. ANL-7130 (unpublished), p. 115; Lawrence Radiation Laboratory Report No. UCRL 16473 (1965) (unpublished).

<sup>26</sup> R. H. Dalitz, Proc. Phys. Soc. (London) A69, 527 (1956).

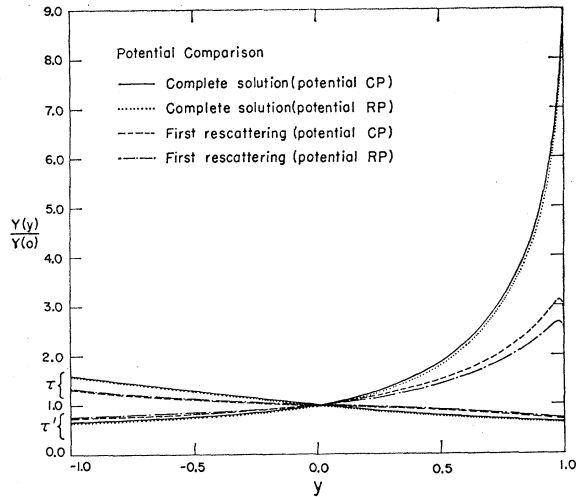


FIG. 6. The normalized decay spectra  $Y(y)/Y(0)$  for  $a_0 = 4.22 m_\pi^{-1}$  and a bound state at  $1.91 m_\pi$ ,  $a_2 = -0.8 m_\pi^{-1}$ ,  $r_2 = 2.0 m_\pi^{-1}$ , no  $I=1$  amplitude, and  $A=0$ .

$y=1$  in Fig. 6 is due to the square-root singularity at the two-pion threshold and was pointed out by Sawyer and Wali.<sup>3</sup> It is present in most of our curves, although it is not always noticeable.

It should be pointed out that although the shapes of the spectra seem to be insensitive to the shape of the potential, the absolute rates are not, as can be seen in Table I. This is just a reflection of the different cutoffs provided by the potentials. The potential which has a  $1/r$  dependence (RP) near  $r=0$  produces a larger rate than the potential which goes to a constant at the origin (CP). Thus there may be cases (for example, repulsive potentials—see end of Sec. IV.B) where the sensitivity of the spectra to the potential shape is much greater than we have found. This important point deserves more study. However, this limited comparison of potentials

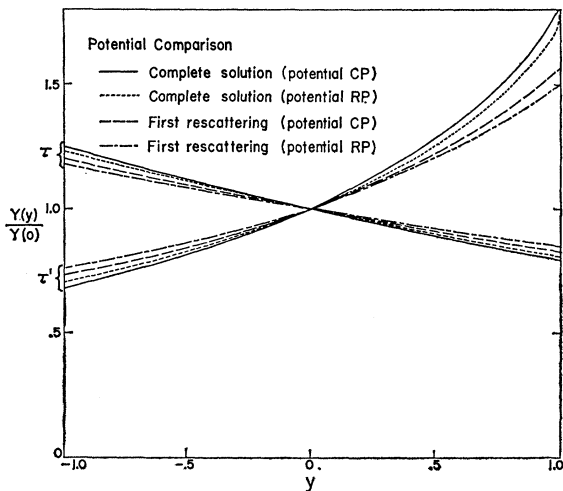


FIG. 7. The normalized decay spectra  $Y(y)/Y(0)$  for  $a^0 = -0.8 m_\pi^{-1}$ ,  $r_0 = 2.0 m_\pi^{-1}$ , no  $I=1$  or  $2$  amplitudes, and  $A=0$ .

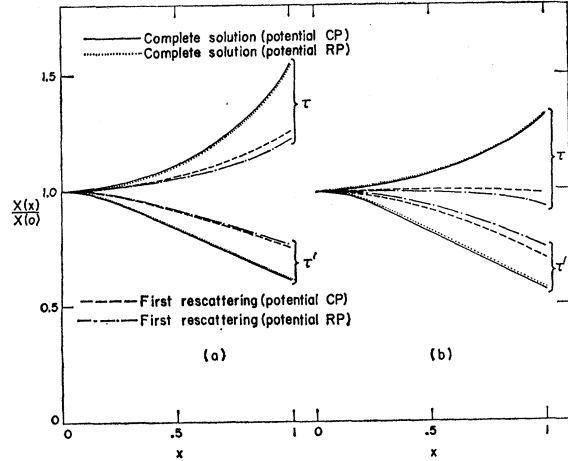


FIG. 8. The normalized decay spectra  $X(x)/X(0)$  for the same parameters as in Fig. 5 for graph (a) and Fig. 6 for graph (b). Only the region  $x > 0$  is plotted since the spectra are necessarily even in  $x$ . The spectra corresponding to the parameters in Fig. 7 have a small slope.

leads us to believe that for most cases the spectrum shapes we obtain with the potential CP will be close to those obtained with more complicated potentials.

The pion-pion scattering amplitudes considered here are clearly inconsistent with the experimental data, having the wrong sign of the slope in the  $y$  variable and too much dependence on  $x$ .

## B. Comparison with Khuri-Treiman Approximation

Using a zero-range model for the  $S$ -wave pion-pion scattering amplitudes and a once subtracted relativistic dispersion relation, Khuri and Treiman<sup>1</sup> related the  $\tau$ -decay spectrum to the difference between the  $I=0$  and  $I=2$  scattering lengths,  $a_0$  and  $a_2$ . Their formula is

$$|M(x,y)|^2 \approx 1 + \frac{5\rho^2}{3\pi(1+\frac{1}{2}\rho^2)^{1/2}}(a_0 - a_2)y, \quad (4.8)$$

where  $\rho^2 = \frac{1}{3}Em_K$  is a kinematical factor equal to 0.64.

TABLE I. The absolute decay rates in units of  $H^2$  calculated from the first rescattering approximation ( $R_1$ ) and the complete solutions ( $R_c$ ) for the potentials CP and RP.

		$R_1\tau$	$R_c\tau$	$R_1\tau'$	$R_c\tau'$	$R_c\tau/R_c\tau'$
$a_0 = 4.22m_\pi^{-1}$ ; $m_{BS} = 1.91m_\pi$ ; no $I=2$ potential	CP	8.15	6.92	2.68	1.93	3.58
	RP	26.36	51.20	8.59	14.20	3.60
$a_0 = 4.22m_\pi^{-1}$ ; $m_{BS} = 1.91m_\pi$ ; $a_2 = -0.8m_\pi^{-1}$ ; $r_2 = 2.0m_\pi^{-1}$	CP	11.70	12.63	3.66	3.65	3.46
	RP	36.00	173.3	10.21	49.80	3.48
$a_0 = -0.8m_\pi^{-1}$ ; $r_0 = 2.0m_\pi^{-1}$ ; no $I=2$ potential	CP	4.38	5.54	1.14	1.41	3.94
	RP	10.38	18.40	2.68	4.38	3.95
No final-state interaction			0.8376	0.2094		4

(Note that our sign convention for the scattering lengths is opposite to that of Khuri and Treiman, so that  $a_I < 0$  corresponds to an attractive potential.) However, their derivation depends on a cutoff due to relativistic kinematics. Since our formula is nonrelativistic, the corresponding cutoff is provided in a different manner and therefore results cannot be compared directly. With this in mind we derive from our equations the nonrelativistic analog of the Khuri-Treiman matrix element.

Equation (3.1) for  $W(q, I)$  can be subtracted at  $q=q_0=\sqrt{\frac{2}{3}E}$ , the center of the Dalitz plot. The integral equation for the difference function  $W(q, I) - W(q_0, I)$  converges even in the limit of constant potential, i.e.,  $\beta \rightarrow \infty$ . If the limits  $\beta \rightarrow \infty$  and  $\lambda \rightarrow \infty$  are taken in such a way that the scattering length stays finite, one can obtain equations for the functions  $U(\mathbf{k}, q, I)$  introduced in Eq. (1.21):

$$U(\mathbf{k}, q, I) = U(q, I) = U(q_0, I) + \Phi(q, I), \quad (4.9)$$

where

$$\Phi(q, I) = \frac{a_I}{1 + i\bar{q}a_I} \left[ (i\bar{q}_0 - i\bar{q})G(I) + \sum_J R(I, J) \int_0^\infty [\Delta(q, q') - \Delta(q_0, q')] \Phi(q', J) dq' \right]; \quad (4.10)$$

$$\Delta(q, q') = \frac{1}{\pi} \frac{q'}{q} \ln \left( \frac{E - q^2 - q'^2 - qq' + i\epsilon}{E - q^2 - q'^2 + qq' + i\epsilon} \right), \quad (4.11)$$

and

$$G(I) = H_w(I) + U(q_0, I) + \sum_J 2R(I, J)U(q_0, J) \quad (4.12)$$

is proportional to the decay amplitude at the center of the Dalitz plot.

These equations are identical to Eqs. (17) and (24) of Anisovich<sup>22</sup> except that the subtraction point is at the center of the Dalitz plot. (Anisovich also uses  $\bar{q}$  instead of  $q$  as the integration variable.) The connection between the Khuri-Treiman and Anisovich equations is discussed in Ref. 13.

In the spirit of Khuri and Treiman we find an approximate solution by taking only the inhomogeneous term (first rescattering term) of this *subtracted* equation. We thus obtain for the matrix elements for  $\tau$  and  $\tau'$  decay

$$\begin{aligned} M_\tau &= 1 + D(k_3, a_2) + \frac{1}{6} [D(k_1, a_2) + D(k_2, a_2)] \\ &\quad + \frac{5}{6} [D(K_1, a_0) + D(k_2, a_0)], \\ M_{\tau'} &= -\frac{1}{2} + \frac{1}{3} D(k_3, a_2) - \frac{5}{6} D(k_3, a_0) \\ &\quad - \frac{1}{2} [D(k_1, a_2) + D(k_2, a_2)], \end{aligned} \quad (4.13)$$

where

$$D(k_i, a_I) = (k_0 - k_i) a_I / (-i + k_i a_I), \quad (4.14)$$

and  $k_0 = \sqrt{\frac{1}{3}E}$  is the value of  $k_i$  ( $=\bar{q}_i$ ) at the center of the Dalitz plot. These simple expressions predict a

slope at the center of the Dalitz plot for  $\tau$  decay of

$$\frac{5}{6} k_0^2 \{ a_2^2 / (1 + k_0^2 a_2^2) - a_0^2 / (1 + k_0^2 a_0^2) \}, \quad (4.15)$$

which differs from expression (4.8) in that it depends only on the squares of the scattering lengths.

Cusps due to the square-root singularities at the two pion thresholds, such as those noted in Sec. IV.A, will arise from the explicit appearance of  $(k_0 - k_i)$  in Eq. (4.14).

Although we have not solved Eq. (4.10) we expect that for potentials having a short range the solution to Eqs. (3.15)–(3.16) will be very similar to the solution of Eq. (4.10). In Figs. 9 through 15 we show the results for the complete solution to Eqs. (3.15)–(3.16), the single rescattering or inhomogeneous term of Eq. (3.16), and the approximate formula, Eq. (4.13). In all of these cases, parameters were chosen to make

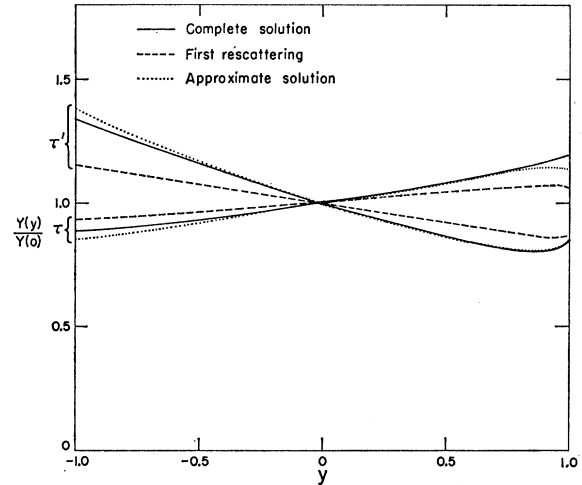


FIG. 9. The normalized decay spectra  $Y(y)/Y(0)$  for  $a_0 = -0.3 m_\pi^{-1}$ ,  $a_2 = -1.0 m_\pi^{-1}$ , zero effective range, and  $A = 0$ .

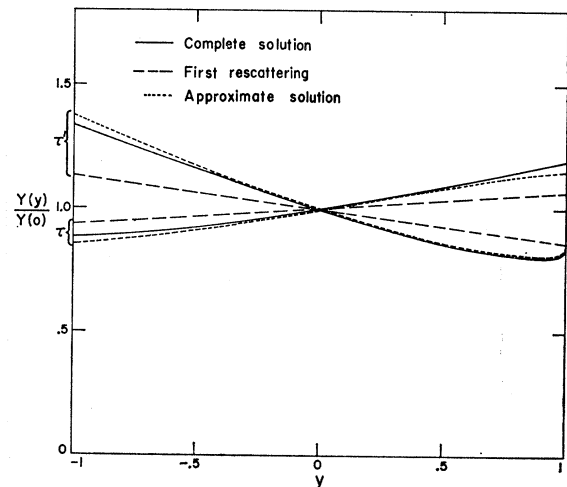


FIG. 10. The normalized decay spectra  $Y(y)/Y(0)$  for  $a_0 = +0.3 m_\pi^{-1}$ ,  $a_2 = +1.0 m_\pi^{-1}$ , zero effective range, and  $A = 0$ .

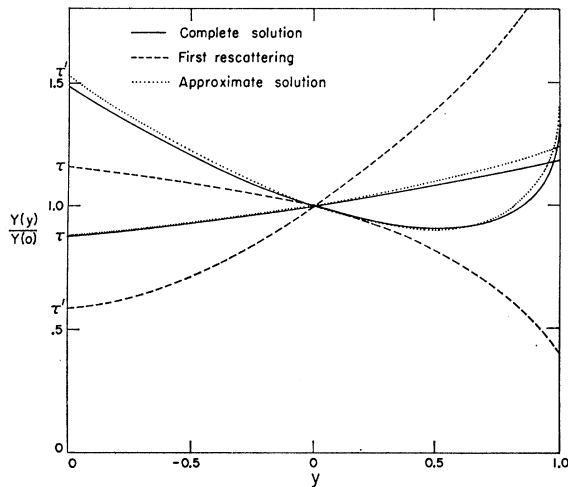


FIG. 11. The normalized decay spectra  $Y(y)/Y(0)$  for  $a_0 = +0.3 m_\pi^{-1}$ ,  $a_2 = -1.0 m_\pi^{-1}$ , zero effective range, and  $A = 0$ .

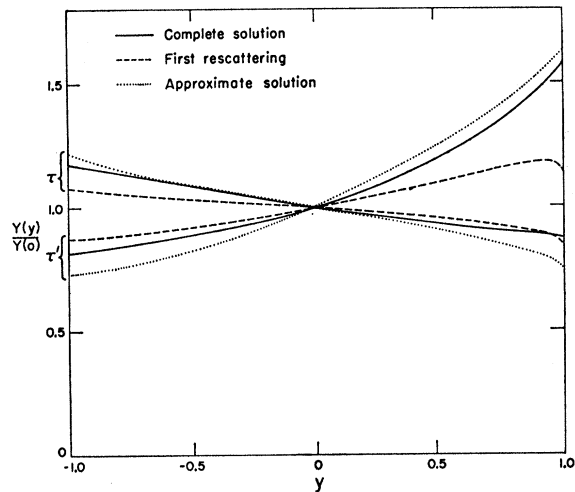


FIG. 13. The normalized decay spectra  $Y(y)/Y(0)$  for  $a_0 = -1.5 m_\pi^{-1}$ ,  $a_2 = -0.8 m_\pi^{-1}$ , zero effective range, and  $A = 0$ .

the effective ranges zero. The spectra  $X(x)$  are essentially constant and are not shown.

The first conclusion to be drawn from these results is that the single rescattering term is not a good approximation to the complete solution. This is especially noticeable in Fig. 11, where it even leads to the wrong sign in the slope. The reason for this is that the homogeneous term in the integral equation is much larger than the inhomogeneous term, as can be seen from the relative rates in Table II.

On the other hand, when the equation is "renormalized" by making one subtraction the resulting inhomogeneous term does provide a good approximation, i.e., Eq. (4.13), for small scattering lengths as was argued by Khuri and Treiman. As the scattering length becomes larger in magnitude, the real or virtual bound-state pole in  $\tau(\bar{q}, I)$  at  $\bar{q} = i/a_I$  moves closer to the Green's-

function singularity of the kernel so that it is no longer a good approximation to replace  $W(q', I)$  by a constant inside the integral of Eq. (3.1) which is an alternative way of obtaining Eq. (4.13).

Thus, for attractive potentials, the multiple scattering does not change the sign of the slope from what has been found previously, i.e., to fit the experimental data one needs  $|a_0| < |a_2|$  (Figs. 12 and 13). The approximate form for the slope, Eq. (4.15), predicts that  $(a_2^2 - a_0^2) \sim 2$  would fit the data. This contradicts what is generally expected for the scattering lengths, namely,  $a_2$  small and  $a_0$  large and negative.<sup>9</sup>

Chew<sup>24</sup> has suggested that  $a_0$  might be positive because of a fictitious bound state in the  $I=0$  pion-pion system. To investigate this possibility in the context of our potential model we chose a scattering length of  $+0.3$  corresponding to a binding energy of  $11 m_\pi$ .

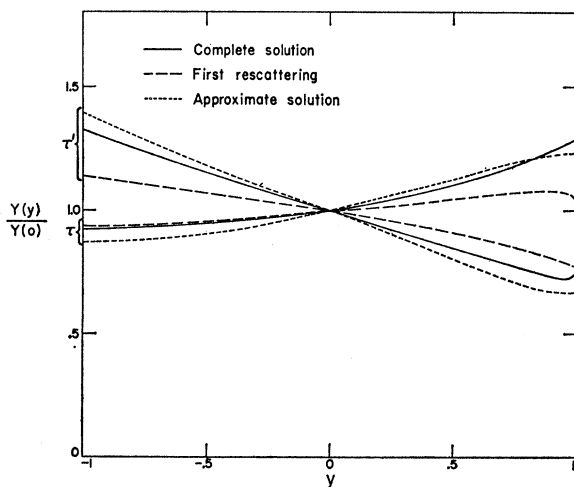


FIG. 12. The normalized decay spectra  $Y(y)/Y(0)$  for  $a_0 = -0.8 m_\pi^{-1}$ ,  $a_2 = -1.5 m_\pi^{-1}$ , zero effective range, and  $A = 0$ .

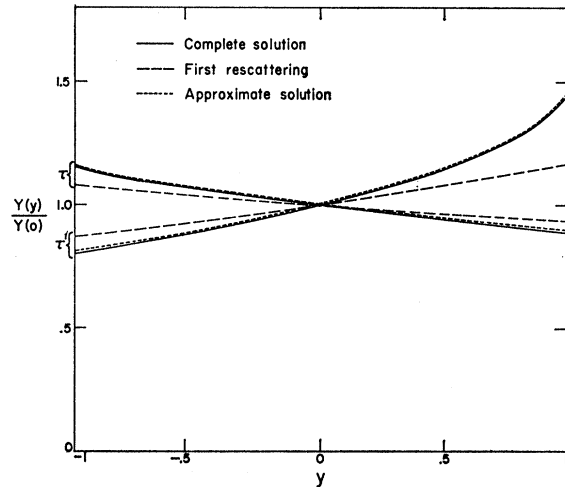


FIG. 14. The normalized decay spectra  $Y(y)/Y(0)$  for  $a_0 = +0.8 m_\pi^{-1}$ , no  $I=2$ , zero effective range, and  $A = 0$ .

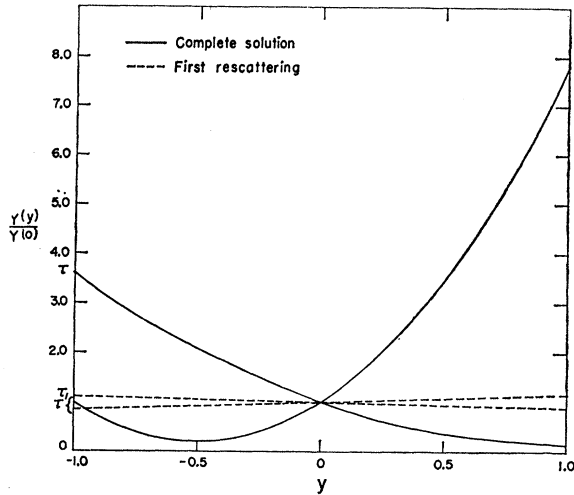


FIG. 15. The normalized spectra  $Y(y)/Y(0)$  for a repulsive potential,  $a_0 = +0.8 m_\pi^{-1}$ , no  $I=2$ , zero effective range, and  $A=0$ . The spectra corresponding to the approximate solution, Eq. (4.13), are the same as those in Fig. 14.

Results are shown in Fig. 11. It is quite likely that a fit to the data could be found but it would still require  $|a_0| < |a_2|$ .

Our results differ from those of Khuri and Treiman<sup>1</sup> in that the slope is independent of the sign of  $a_I$ , as can be seen by comparing Figs. 9–11. Khuri and Treiman did not actually consider bound states in their formalism, since no bound dipion is known. They did, however, assume Eq. (4.8) to be valid for repulsive interactions. Our Eq. (4.13) predicts that repulsive potentials and potentials attractive enough to produce a bound state should have the same Dalitz plot if they have the same scattering length. Comparison of Figs. 14 and 15 shows that this does not apply to the complete solution. The reason can be seen in the relative rates in Table II. A repulsive interaction is expected to decrease the rates. This decrease shows itself as a cancellation between the pure weak matrix element and the rescattering terms in Eq. (4.3). This effect is already

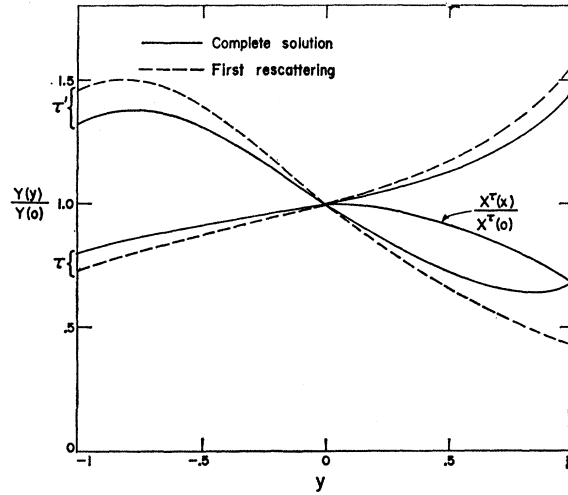


FIG. 16. The normalized spectra  $Y(y)/Y(0)$  for an  $I=0$  resonance of mass 357 MeV and width 86 MeV, no  $I=1$  or 2 amplitudes, and  $A=0$ .

apparent with the inclusion of only the first rescattering term. With the multiple rescattering included the cancellation is almost complete in the physical region for the parameters chosen. In fact, at one point the real part of the matrix element goes through zero while the imaginary part remains small. Since the final spectra depend sensitively on this cancellation, the shape of the Dalitz plot shown in Fig. 15 could be dependent upon the choice of potential.

### C. Resonances

All of the zero-range curves are linear near  $y=-1$ . Some of the data<sup>28</sup> on the  $K_2^0 \rightarrow \pi^+\pi^-\pi^0$  decay show a maximum near  $y=-0.8$ . A fit to this maximum could be obtained by assuming an  $I=0$  resonance of mass  $\sim 357$  MeV and width 86 MeV. (See Fig. 16.). However, these parameters do not fit the  $\eta \rightarrow \pi^+\pi^-\pi^0$  spectra. If the mass is increased to fit the  $\eta$  spectra, no maximum would appear in the  $K_2^0$  spectrum. Our results are equivalent to those of Brown and Singer.<sup>6</sup> This is due

TABLE II. The absolute decay rates in units of  $H^2$  calculated from the first rescattering approximation and the complete solution for some zero-range cases.

	$R_1\tau$	$R_c\tau$	$R_1\tau'$	$R_c\tau'$	$R_c\tau'/R_c\tau'$
$a_0 = +0.3m_\pi^{-1}; a_2 = +1.0m_\pi^{-1}$	$6.39 \times 10^2$	$9.19 \times 10^3$	$1.60 \times 10^2$	$2.32 \times 10^3$	3.96
$a_0 = +0.3m_\pi^{-1}; a_2 = -1.0m_\pi^{-1}$	$8.10 \times 10^1$	$8.02 \times 10^3$	$2.08 \times 10^1$	$2.10 \times 10^3$	3.82
$a_0 = -0.3m_\pi^{-1}; a_2 = -1.0m_\pi^{-1}$	$7.80 \times 10^2$	$1.85 \times 10^6$	$1.95 \times 10^2$	$4.69 \times 10^5$	3.94
$a_0 = -0.8m_\pi^{-1}; a_2 = -1.5m_\pi^{-1}$	$6.53 \times 10^2$	$8.44 \times 10^4$	$1.64 \times 10^2$	$2.13 \times 10^4$	3.96
$a_0 = -1.5m_\pi^{-1}; a_2 = -0.8m_\pi^{-1}$	$6.28 \times 10^2$	$6.41 \times 10^4$	$1.57 \times 10^2$	$1.61 \times 10^4$	3.98
$a_0 = +0.8m_\pi^{-1}$ ; attractive	$1.79 \times 10^2$	$2.01 \times 10^3$	$4.51 \times 10^1$	$5.11 \times 10^2$	3.93
$a_0 = +0.8m_\pi^{-1}$ ; repulsive	$1.81 \times 10^{-1}$	$6.25 \times 10^{-4}$	$4.55 \times 10^{-2}$	$2.40 \times 10^{-4}$	2.60
No final-state interaction		0.8376		0.2094	4

<sup>28</sup> P. Basile *et al.*, in Proceedings of the Argonne International Conference on Weak Interactions, 1965, Argonne National Laboratory Report No. ANL-7130 (unpublished), p. 77.

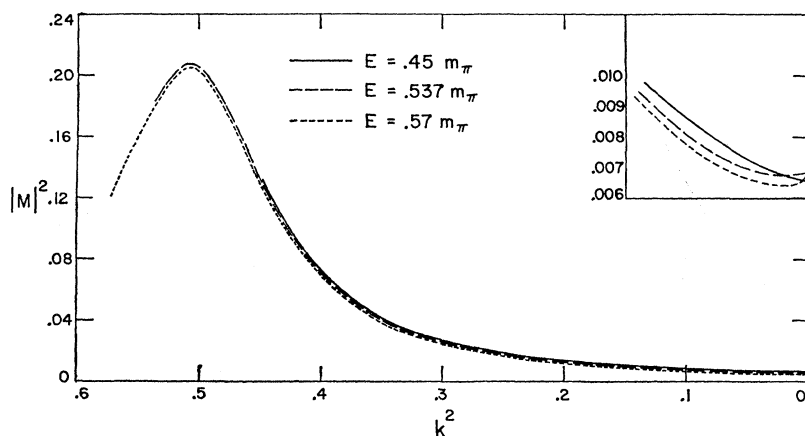


FIG. 17. The square of the matrix element for  $\tau'$  decay plotted as a function of the  $\pi^0-\pi^0$  relative energy  $k^2$  at three different values of  $E$ . The  $I=0$  pion-pion resonance is at 350 MeV with a width of 21 MeV. There is no  $I=1$  or 2 amplitude, and  $A=0$ . The small  $k^2$  region, where the effect of the triangle singularity would appear, is also shown on an expanded scale.

to the dominance of the resonance pole which makes the complete solution nearly proportional to the first re-scattering term.

In Fig. 16 we have also plotted the  $X(x)$  spectrum for  $\tau$  decay because in the presence of a resonance  $X(x)$  may show appreciable departure from being constant. This should be considered when fitting a resonance form to the data. It is also important to include the momentum dependence of the width of the resonance.

We also looked for effects<sup>13</sup> of the triangle singularity of diagrams such as that in Fig. 4. In order to bring the triangle singularity close to the physical region, the resonance should have a narrow width. However, the strength of the singularity is proportional to the width, so a compromise width of 21 MeV was chosen. The total kinetic energy  $E$  was varied in order to move the position

of the triangle singularity relative to the physical region. Results are shown in Fig. 17. The triangle singularity should appear as an  $E$ -dependent structure near the  $k^2=0$  end. No effect distinguishable from the square-root singularity at  $k^2=0$  is observed. There is also no effect on the absolute magnitude, as can be seen from the fact that the three curves use the same ordinate scale.

Further calculations, with the inclusion of the  $\rho$  resonance in the  $T=1, l=1$  pion-pion scattering amplitude and the linear term  $A$  of the weak interaction, are being performed.

#### ACKNOWLEDGMENT

The authors wish to thank L. Mather for help with some of the numerical calculations.